Design and Test of a Reluctance Based Magnetic Lead Screw PTO System for a Wave Energy Converter

Nick Ilsø Berg*, Alexander Becsei Christiansen, Rasmus Koldborg Holm and Peter Omand Rasmussen
Department of Energy Technology
Aalborg University, Aalborg, Denmark
*Email: nib@et.aau.dk

***Abstract*—Abstract—This paper deals with the design and test of a Reluctance based Magnetic Lead Screw Power Take Off (PTO) system for a Wave Energy Converter for powering a LED light buoy. In order to meet the power requirement for the LED marking light, measurements of the seastate at the specific location of the buoy is carried out using a special wave measurement buoy. The data is used to set up a simulation model of the possible harvested energy using a Magnetic Lead Screw (MLS) as the core component of the PTO system. Specifications of the MLS generator, in terms of stall force, lead, stroke etc. are found based on these simulations. Design of the MLS unit is carried out using FEM models of the MLS magnetic circuit, together with mechanical design consideration for minimizing the total cost of the device. Test of efficiency and stall force of the built prototype is carried out and presented.**

***Index Terms*—Permanent Magnet, PMSM, Wave Energy Converter, Power TakeOff System, FEM, Simulation, Magnetic Lead Screw, Reluctance**

I. Introduction

Today, many hours of service is spend on ocean marking lights, for instance for fish farms. The service include change of batteries for powering the LED marking light, which is done by technicians using a service vessel for each buoy. The process of changing batteries is expensive and time consuming why other technologies are investigated. One of theese new technologies is the idea of having a LED marking buoy which is self-powered, which should minimize the requirement for servicing. Until now, the most popular technology for self-powering buoys is PhotoVoltaics (PV) panels. However one drawback using PV panels for ocean buoys, is problems with salt crystalizing on top of the panels, which decrease the efficiency of the panels dramatically, as seen in the work done in [1] and [2]. Another solution is to install a Wave Energy Converter (WEC) which converts the linear movement of the buoy due to incoming waves into electricity. This paper deals with the development of a Magnetic Lead Screw (MLS) as the core component in the Power Take Off System (PTO) in the WEC, which should be able to power a LED marking light. An overview of the different components of the WEC is depicted in Figure 1.

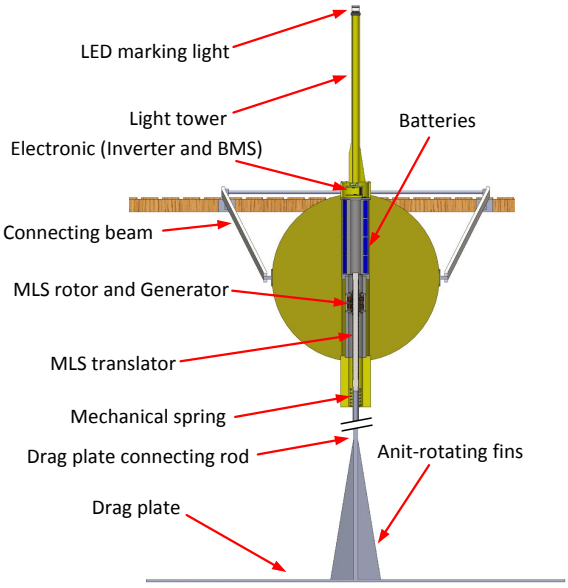

Fig. 1. Mechanical overview of buoy

The LED marking light is located at the top of the device in order to maximize the visible range. In top of the buoy all the electronic components are gathered, which is the control board for the LED light, the inverter for the generator and Battery Management System (BMS) for the batteries. The batteries are used to level out the power production of the WEC, and to power the LED light at calm weather with zero or small incoming waves. The calculation of batterie size and

The development of the PTO system is financial supported by Ocean Energy A/S.

978-1-5090-4281-4/17/$31.00 ©2017 IEEE.

type is beyond the scope of this paper, and will be presented when the full WEC has been tested at open sea in a later paper. The batteries however are placed in the outer shell of the translator cylinder, in order to keep the center of gravity near the bottom of the float while not having the batteries beneath the water surface, which would minimize the risk of seepage of water into the fully sealed battery container. The MLS which is located in the center of the float, is part of the PTO system, that converts the slow linear movement of the waves into a fast rotating movement of a rotor, which makes it possible to extract energy using a standard rotary generator, as described in [3]. The MLS consist of a translator and rotor, where the translator moves linearly while the rotor rotates with a speed determined by the lead of the MLS and the input linear velocity. The MLS uses helically shaped magnets in order to transfer the linear force of the translator into a torque working on the MLS rotor. The use of magnets makes it possible for the MLS to slip one or more pole pairs if the force applied to the translator exceeds the stall force of the MLS, i.e. the maximum force the MLS is capable of transferring. This capability makes the MLS very suitable for WEC compared to mechanical geared systems, as any big waves will not damage the MLS and/or the generator of the PTO of the WEC. The rotor of the MLS is attached to a PMSM machine, which converts the rotary movement of the MLS rotor into electricity while the translator of the MLS is attached to a submerge dragplate, which tends to keep the translator stationary while the float of the WEC moves according to the incoming wave [4]. This paper is organized in five sections, where the first section is this introduction followed by a brief explanation of the simulation model used for sizing the PTO system. In the third section the design of the MLS based upon FEM models of the magnetic circuit is presented, which lead to initial test of the build prototype. Test of the efficiency and stall force capability is presented. Last, a conclusion is given.

II. Simulation

In order to size the PTO system for the WEC in the LED marking light buoy, it is necessary to gather wave data information from the location of the light buoy site together with power consumption of the LED light. This is done using a special wave measurement buoy, which measures the wave height and period of the waves. The measurement buoy was placed at the site for 76 days, from November to January, which was considered representative for the development of

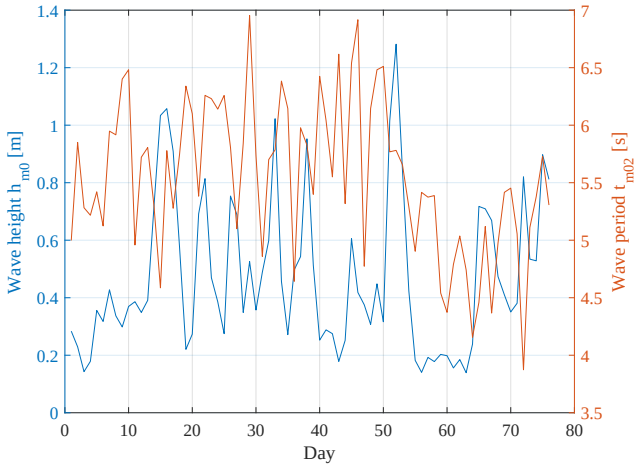

Fig. 2. Measured wavedata

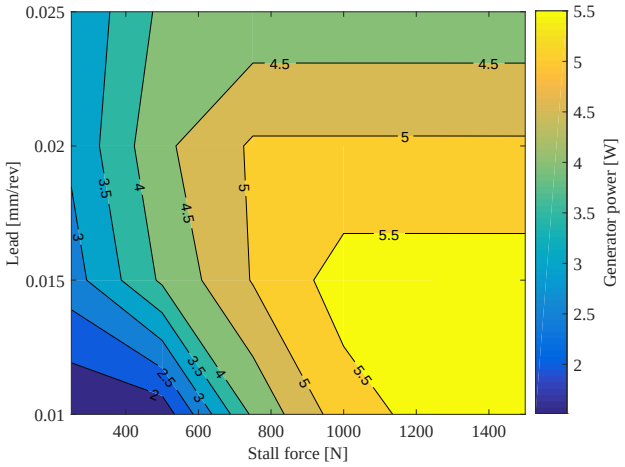

Fig. 3. Contour of harvested energy from simulation results

the prototype. Ideally the measurements should have been performed for a whole year, however this was not possible. Therefore in order to meet a possible low seastate in the summer period, the WEC is designed to produce a minimum of 4 w for the measurement period. The result of the measurement can be seen in Figure 2, in which the significant wave height H_{m0} and mean absolute wave period T_{m02} for each day is depicted. The collected data are used in a developed simulation model of the buoy and generator unit. This model includes a linear wave theory model of the float, a dynamic model of the MLS magnetic spring, the mechanical spring and dragplate, and a loss model of the generator in order to calculate the possible extracted energy. In Figure 4 the simplified mechanical model with interacting forces is shown. In Equation 1 and 2 the equations describing these

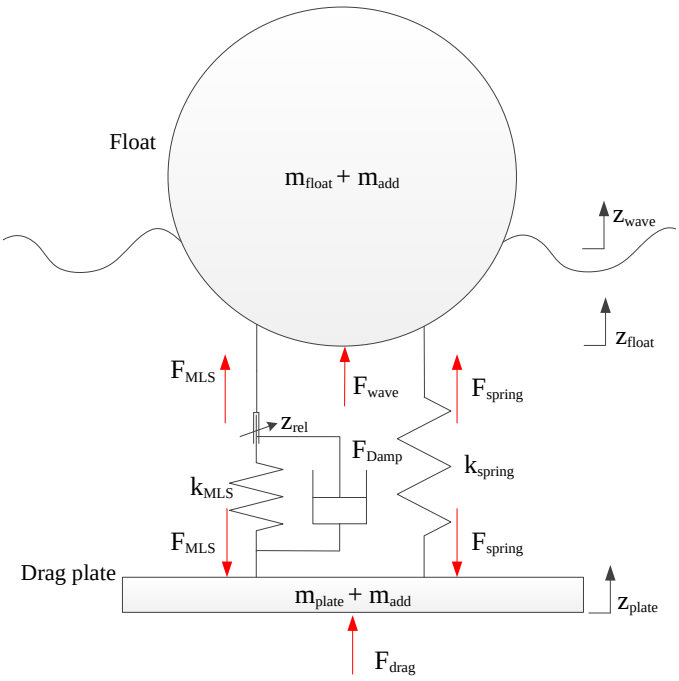

Fig. 4. Mechanical model of WEC

simplified forces are depicted. Z_{float} is the movement of the buoy/float which is a function of both the incoming wave, the mechanical spring force and the force developed by the MLS. The core structure of this functions is a simplified linear wave theory model, based on hydrodynamic parameters of the float estimated using ANSYS AQWA. A detailed describtion of this model is beyond the scope of this paper, why it is treated as a function with three inputs as shown in Equation 1. The force of the MLS is calculated as a sinousidal spring as shown in [3] and again in [5]. The damping strategy is simplified to a constant damping coefficient B_{MLS} which multiplied with the rotor speed, gives the current hence the torque reference for the generator. The simplified loss model of the generator, consist of two loss terms, the copper loss in the armature as a function current, and the iron loss as a function of rotor speed due to eddy current and hysteresis loss.

$$\begin{aligned} Z_{float} &= f(F_{MLS}, F_{spring}, Z_{wave}) \\ F_{MLS} &= F_{stall} \cdot sin(Z_{rel}) \\ F_{spring} &= k_{coilspring} \cdot (Z_{float} - Z_{plate}) \\ F_{Damp} &= \tau_{motor} \cdot (2 \cdot \pi / l_{lead}) \\ F_{drag} &= 0.5 \cdot C_d \cdot \rho_{water} \cdot A_{plate} \cdot \dot{Z}^2_{plate} \\ \tau_{motor} &= k_{motor} \cdot I_{rms} \\ I_{rms} &= \omega_{motor} \cdot B_{MLS} \end{aligned} \tag{1}$$

$$\begin{aligned} P_{copper} &= 3 \cdot R_s \cdot I^2_{rms} \\ P_{iron} &= m_{stator} \cdot \left(k_h \cdot f \cdot \hat{B}^2 + k_c \cdot f^2 \cdot \hat{B}^2 \right) \\ P_{mech} &= F_{Damp} \cdot (\dot{Z}_{float} - \dot{Z}_{plate}) \\ P_{elech} &= P_{mech} - P_{copper} - P_{iron} \end{aligned} \tag{2}$$

The simulation model serves the purpose of determine the appropriate parameters of the MLS generator and the size of the dragplate together with the battery size, in order to extract enough energy to power the LED marking light. The battery and dragplate sizing are not within the scope of this paper, and will be presented in a later paper. Due to restriction in the manufacturing process, the float/buoy is fixed to a sphere having a diameter of 1 m. A parameter sensitivity study of the extracted energy of the WEC, are carried out by performing parameter sweeps as depicted in Figure 3. The result of the sweep when changing stall force and lead clarifies the need of optimal parameter configuration in order to size the WEC appropriate. Based on several sweeps not shown in this paper, the MLS is build with a lead of 14 mm/rev and a stall force of 800 N, producing 5 W in average for the 76 days period of the collected wave data.

III. Design

In order to meet the requirements found in the simulation and optimization process, a 2D axissymmetric FEM model calculating the stall force of the MLS is developed and a more thorough mechanical design of the WEC is found based on the results from both the 2D FEM model and the simulation requirements. Due to a fast calculation time of the 2D axissymmetric FEM model, and the fact that the stall force of the MLS, has been analytical and experimental validated several times as shown in [6], [7], and analytical model calculating the stall force has not been developed. When considering the magnetic design of the MLS, previous work in [8] has shown that using a Hallbach Array (HA) orientation of the NdFeB magnets enhance the utilization of the magnets in the MLS. Additional work in [9] connect the work done in [8] with a PMSM motor for increasing the compactness of the device. In this paper a new reluctance type MLS with hallbach array magnets on the rotor part and a steel thread as the translator part, Hallbach Array Reluctance (HAR) is proposed. This should further increase the utilization of the magnets, hence lower the cost of the device, as the stroke for the WEC MLS compared with the active length is relative long. The

proposed design is compared with radially magnetized surface mounted (RMSM) type using bonded NdFeB magnets, in order to maintain the cost of the device low. It could be argued that using Ferrite magnets could lower the cost of the device even further, however using ferrite magnets will decrease the stall force of the device with a factor of around 16 as the remanence of ferrite magnets is a factor of 4 lower than that of NdFeb. This would increase the active length of the device with a factor of 16, hence the generator unit is not increased why this would lead to a increase in material usage and thereby cost of the device. In Figure 5 and 6the two designs with radially magnetized bonded NdFeB and hallbach array sintered NdFeB magnets are presented.

As indicated in [8] the RMSM has a low stall force saturation level, hence a magnet thickness of above 4 mm will not increase the stall force of the MLS significantly. On the contrary the HAR magnetic design has a high force saturation level, with a maximum magnet thickness of around 8-9 mm. As explained previously the WEC MLS has a large ratio between stroke and active rotor length, which means that the most of the magnets on the translator is not engaged, hence the utilization of the NdFeB material is very low. This could be solved using a very long rotor compared to the stroke, which would decrease the ratio. However this would require a long and slender rotor, which for the particular design and performance specifications is impractical to build.

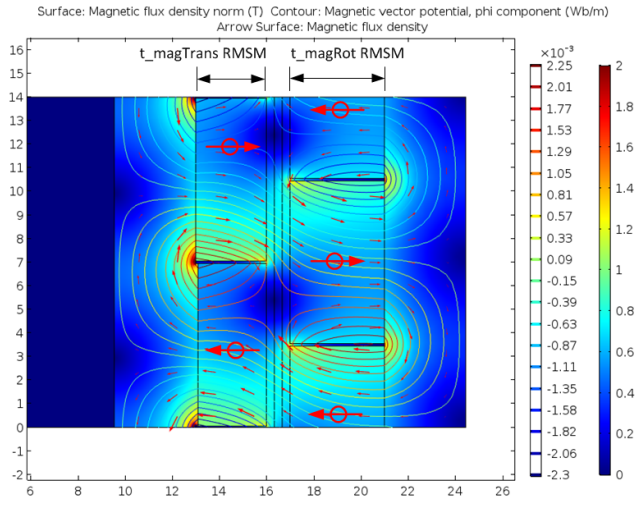

Fig. 5. Flux density plot of radially magnetized bonded NdFeB type MLS

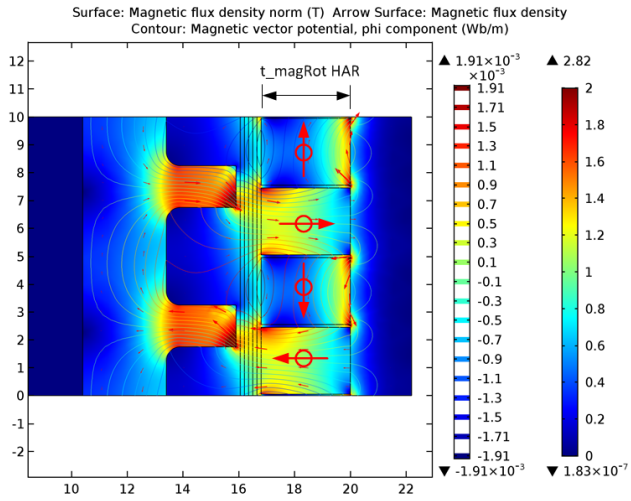

Fig. 6. Flux density plot of Hallbach array reluctance type MLS

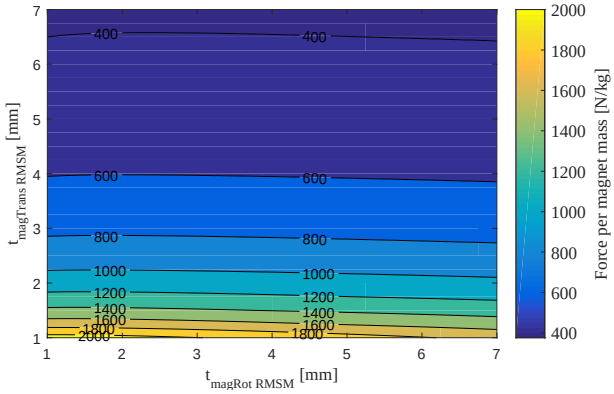

Fig. 7. Force per magnet mass of RMSM vs magnet thickness on both rotor and translator

In Figure 7 and 8 the force per magnet mass is depicted as a function of magnet thickness. The diameter and airgap for the two simulations are the same (32 mm diameter and 1.0 mm airgap), however the rotor length has been scaled in order to achieve 800 N of stall force for the given magnet thickness. For the HAR design, the highest force per magnet mass (3644 N/kg) is attained at a magnet thickness of 2 mm and a rotor length of 135 mm. As a comparison Kouhshahi et. al recently proposed a design of a magnetically geared lead screw with a force per magnet mass of 900 N/kg [10]. As seen in Figure 7 the highest utilization of the magnets in a RMSM design is reached at low magnet thickness on the translator and at low magnet thickness on the rotor as predicted.

The highest force per magnet mass at approx. 2080 N/kg of the RMSM design is attained with a rotor and translator magnet thickness of 1 mm with a rotor length of 180 mm,

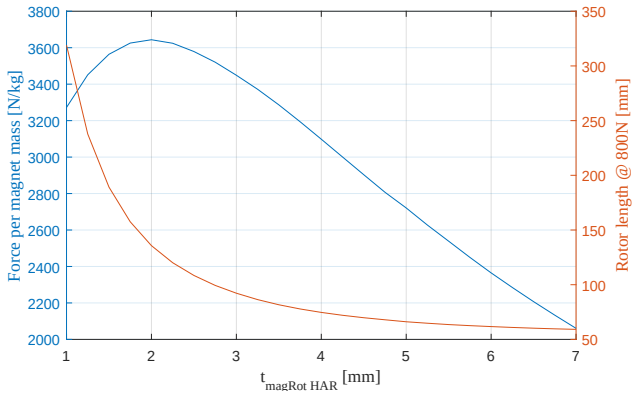

Fig. 8. Force per magnet mass of HAR design vs magnet thickness and rotor length at 800 N stallforce

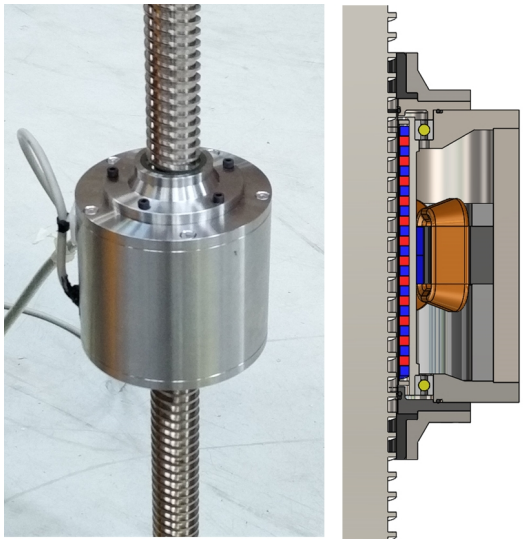

Fig. 9. Final assembled MLS generator prototype and CAD cut through

however the configuration is almost impractical to construct due to the small magnets on the translator and rotor and a rotor length. For a direct comparison of the HAR and RMSM design, the rotor length is chosen to be maximum 140 mm, which for the RMSM design reveal a force per magnet mass of maximum 2069 N/kg, which is 1.7 times lower than for the HAR design. However as the cost of the Bonded NdFeB is lower than the cost of the sintered NdFeB magnets, this most be taken into account together with the mechanical construction of the WEC. In [11] the cost of raw NdFeB N30UH sintered magnets and NdFeB MF25 bonded magnets are stated as 21.82 $/kg and 12.27 $/kg respectively, which converted to the two designs in this paper is 167 N/$ for the sintered NdFeB and 169 N/$ for the bonded type. However the construction of the RMSM bonded

MLS Parameters	**Value**
Lead	14 mm/rev
Stall force	800 N
Force per magnet mass	3000 N/kg
Shear force	88.4 kN/m^2
Rotor diameter	32mm
Rotor active length	90 mm
MLS airgap	1.1 mm
MLS rotor inertia	2.61 kg cm^2
MLS eq mass	52 kg

type requires the translator to be manufactured with helically shaped magnets in a length of 640 mm (500 mm stroke + 140 mm active) and a thickness of 1 mm, which could lead to mechanical failures of the magnet. Another concern using magnets on the translator, is corrosion of the magnets and the fact that the magnets would attract any ferro magnetic particles in the water, which could lead to increased friction in the linear bearings. The HAR design requires only a machined translator which can be manufactured using the same techniques as for a normal spindle, and a short rotor which is build using small helically shaped sintered magnets. Additionally it is possible to seal the magnetic rotor from the water, thereby reducing the possibility of dirt gathering at the linear bearing. Considering these observations and the relative small difference in force per magnet price, it is chosen to construct the WEC PTO system with the HAR design. The final design parameters of the MLS generator is shown in Table III.

IV. Test Results

The MLS generator is tested for stall force capacity, friction and efficiency. Finally the full structure of the buoy with the MLS generator installed together with the dragplate, is tested in a Wave tank, which is capable of generating waves with a maximum of 180 mm height.

A. Stall force and friction test

The MLS generator stall force capacity is measured using a 6 axis force/torque transducer mounted on the translator, while the rotor of the motor is locked by applying a DC current of 30 A. Then the translator is moved linearly and the force/torque is measured together with the translator position. As seen in Figure 10, the force/torque peaks exactly at every 7 mm, which corresponds to a lead of 14 mm, as the HAR type is ”double” threaded due to the reluctance of the translator steel. The magnitude of the measured force peaks at -800 N, however the measured force also include the linear friction force between

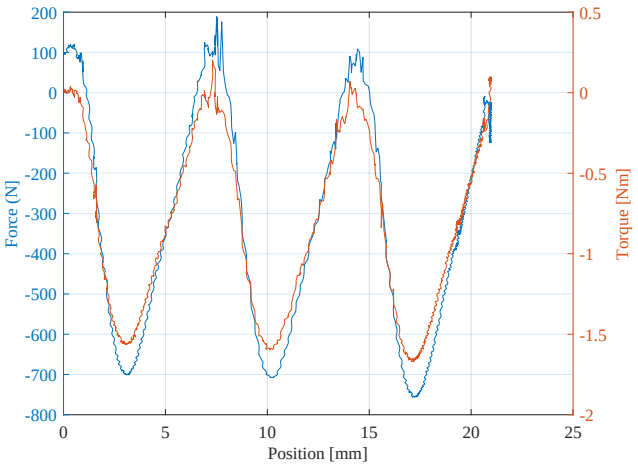

Fig. 10. Stall force test

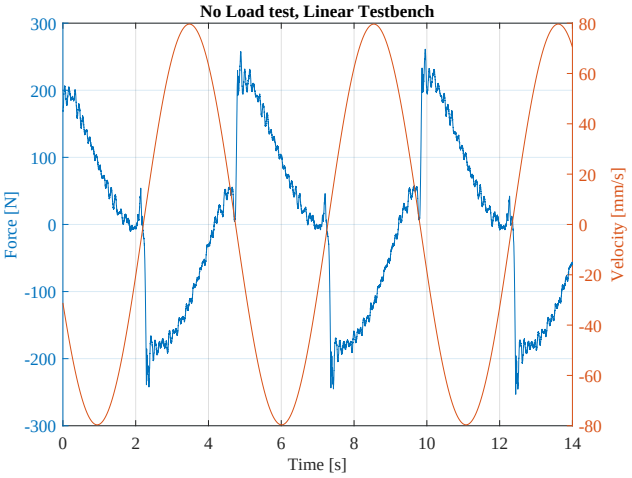

Fig. 12. Linear friction force and velocity at no load conditions

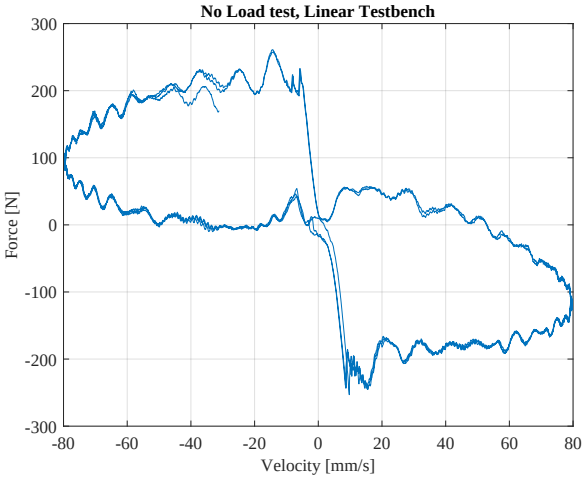

Fig. 11. Force as a function of linear velocity at no load conditions

the translator and the linear bearings. The measured torque however, reflect the MLS stall torque directly, which peaks in -1.58 Nm which converted to a force component using the gearing ratio of the MLS is 709 N, which correspond well with a measured static linear friction of around 100 N. The friction force has also been measured at no load conditions, with a low velocity. The result is presented in Figure 11 and 12.

The reduction of stall force compared to 2D FEM calculations of 800 N, could be due to lower saturation limit of the translator steel, which would greatly affect the stall force. Presently it has not been possible to measure the saturation limit of the steel used for manufacturing of the MLS translator.

B. Efficiency in linear testrig

In order to test the energy harvesting capability of the MLS generator, the device is mounted in a linear test bench, where it is possible to move the translator with a fixed sinusoidal trajectory with different frequencies i.e. velocities. The phase current and voltages of the MLS generator together with DC current and DC voltage from the developed inverter are measured using a power analyser. Additionally a position sensor and force transducer measures the linear velocity and force of the translator, hence it is thereby possible to estimate the mechanical input power. The generator has been controlled as a BLDC generator during these tests, which has proven to be the most beneficial compared to a synchronous Field Oriented Control (FOC) algorithm. This difference could be explained by the frequently occurring direction change of the MLS and low velocity, which cause the position prediction using hall sensors and a prescribed velocity to give faulty positions, which is crucial for the synchronous control algorithm.

The BLDC control however, is of a more robust architecture why the control is not heavily affected by a small error in the position prediction, as the algorithm only uses hall signals for commutation. A more precise position could be implemented by using a high resolution sensor, e.g. resolver or encoder, however this would increase the cost of the device which is not desired. The result of the tests using a BLDC control are depicted in Figure 13 to 15, where the asterisk indicate a measurement point. In Figure 13 the DC power harvested is depicted, which peaks in 18 w when subjected to a sinusoidal trajectory with a RMS linear velocity of 200 mm/s. The overall

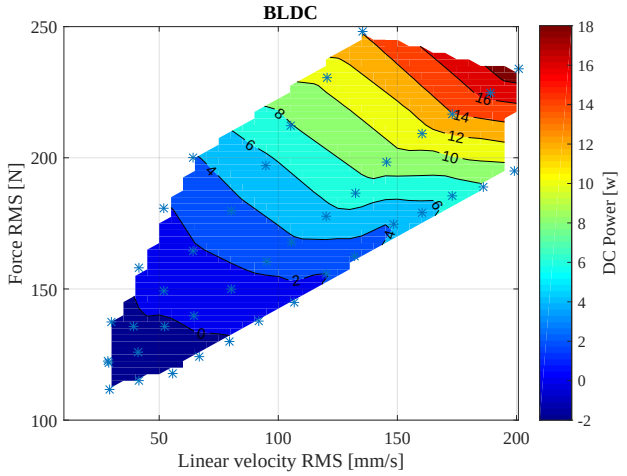

Fig. 13. DC power map of WEC unit as a function of input rms force and linear velocity

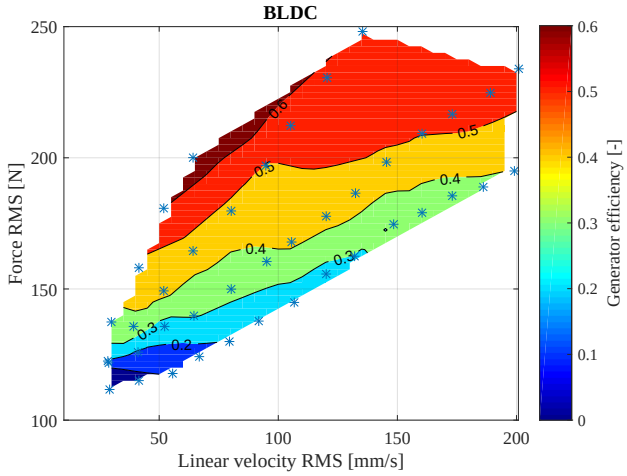

Fig. 14. Generator efficiency map (BLDC)

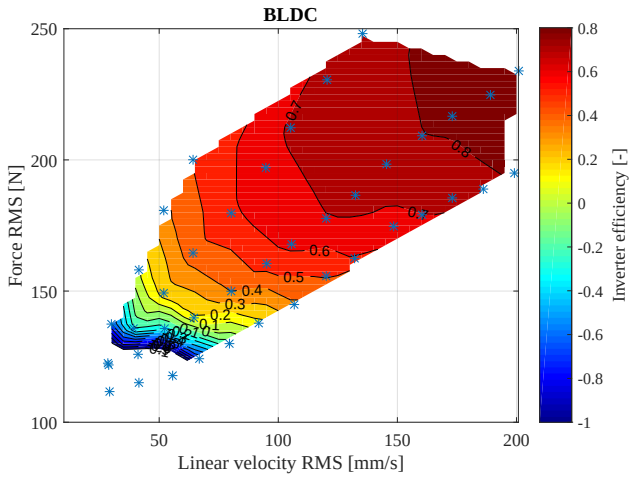

Fig. 15. Inverter efficiency map (BLDC)

system efficiency from mechanical input power to DC power is 50 % at this point, which is relative high considering the high linear friction force of around 100 N.

C. Wave tank test

For model verification and mechanical test of the WEC, the buoy is installed in a wave tank as seen in Figure 16. These test facilities makes it possible to test the buoy at various regular waves with different wave periods and amplitude. Sensors installed in front of the buoy and beside the bouy measures the incoming wave water level, i.e. the wave. A linear sensor mounted in the center of rotation of the buoy, measures the vertical displacement of the buoy when a incoming wave moves the buoy. The diameter of the drag plate connected to the translator was reduced from a diameter of 150 cm found in the previously simulations to 95 cm in order to fit inside the wave tank.

During test in the wave tank, the DC power delivered to the batteries are measured as a function of time, which makes it possible to calculate the mean generated DC power for different damping coefficients. The result of these tests, with a wave period of 2.5 seconds and a amplitude of 180 mm peak-peak (RMS velocity of 113 mm/s), are depicted in 17 together with the simulation result for the same incoming wave.

As evident from Figure 17 the simulation and experimental results correlate up until a damping coefficient of 1000 Ns/m, where the simulation results seems to saturate, additionally the simulation show that choosing a damping coefficient of 1500 or more will result in pole slipping of the MLS, why these results are not present in the Figure. The experimental results however, do not experience pole slipping, nevertheless the DC power generated saturates at 0.7 W @ 1250 Ns/m. The

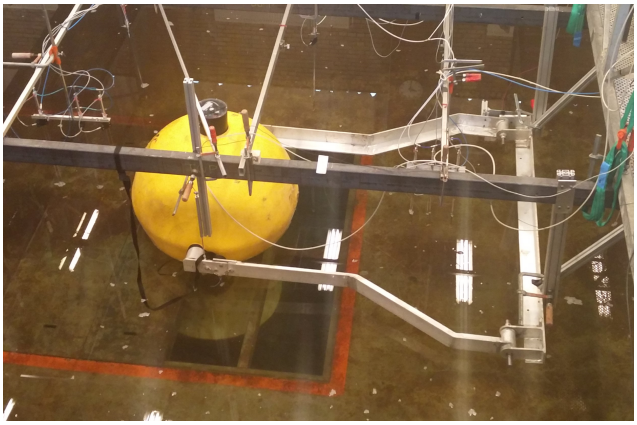

Fig. 16. Buoy installed in Wave tank, for incoming wave test

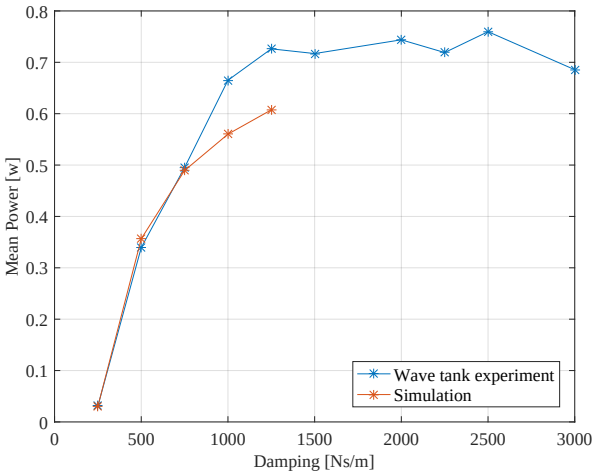

Fig. 17. Experimental simulation results from wave tank

reason for this could be position or velocity depend decrease of drag force, due to small rotation of the buoy which would lead to a skewness of the drag plate and thereby decrease of the drag area and added water mass. Even considering these minor difference between the simulated and measured generated power, the simulation model is recognized as partly validated. In order to validate the full simulation model, it is necessary to run the experiments and simulation model with input waves having a higher amplitude close to the waves measured at the site, see Figure 2.

V. Conclusion

In this paper the design and development of a MLS for a PTO system has been developed. The design of the MLS was based upon models and measurements of the sea state at the specific location, revealing a simulated mean power production of 5 w for a specific configuration of the MLS. The magnetic design of the MLS was based on result found in a developed FEM model of the Hallbach array to reluctance type MLS. The design goal of the MLS stall force was set to 800 N with a lead of 14 mm/rev and an active length of 90 mm. The designed prototype was built and tested, with a measured stall force of 700 N, which was 100 N lower than FEM calculations. The flux saturation level of steel used for the manufactured translator, was proposed as the reason for the lower stall force measured. However measurement of the saturation level has not been carried out prior to this paper, but will be addressed. In order to test the energy harvesting capability of the generator, the efficiency of the prototype was measured in a linear test bench. The sinusoidal cycle efficiency of the MLS generator unit was measured to 50% in a broad working area, with areas having even higher efficiencies. Where the total system efficiency was measured as high as 50% from mechanical input power to electric DC output power. Considering the reciprocating trajectory input, a mean cycle efficiency of 50 % is considered high. The developed simulation model, is validated through test of the buoy in a wave tank, with regular waves as input. The result showed good agreement between the simulated and measured DC power generated. However, test and simulation with input waves having a higher amplitude should be carried out in order to fully validate the simulation model.

References

[1] Y. Sun, X. Yan, C. Yuan, H. Luo, and Q. Jiang, "The i???v characteristics of solar cell under the marine environment: Experimental research," in *2015 International Conference on Renewable Energy Research and Applications (ICRERA)*, Nov 2015, pp. 403–407.

[2] G. Mathiak, J. Althaus, S. Menzler, L. Lichtschlger, and W. Herrmann, "Pv module corrosion from ammonia and salt mist — experimental study with fullsize modules," in *27th European Photovoltaic Solar Energy Conference and Exhibition*, 2012, pp. 3536–3540.

[3] R. K. Holm, N. I. Berg, M. Walkusch, P. O. Rasmussen, and R. H. Hansen, "Design of a magnetic lead screw for wave energy conversion," *IEEE Transactions on Industry Applications*, vol. 49, no. 6, pp. 2699–2708, Nov 2013.

[4] S. Olaya, J. M. Bourgeot, and M. Benbouzid, "Modelling and preliminary studies for a self-reacting point absorber wec," in *2014 First International Conference on Green Energy ICGE 2014*, March 2014, pp. 14–19.

[5] S. Pakdelian, M. Moosavi, H. A. Hussain, and H. A. Toliyat, "Control of an electric machine integrated with the trans-rotary magnetic gear in a motor drive train," *IEEE Transactions on Industry Applications*, vol. 53, no. 1, pp. 106–114, Jan 2017.

[6] J. Wang, K. Atallah, and W. Wang, "Analysis of a magnetic screw for high force density linear electromagnetic actuators," *IEEE Transactions on Magnetics*, vol. 47, no. 10, pp. 4477–4480, Oct 2011.

[7] J. Wang, G. W. Jewell, and D. Howe, "A general framework for the analysis and design of tubular linear permanent magnet machines," *IEEE Transactions on Magnetics*, vol. 35, no. 3, pp. 1986–2000, May 1999.

[8] R. K. Holm, N. I. Berg, and P. O. Rasmussen, "Magnetic design consideration of a magnetic lead screw with halbach array," in *Linear Drives for Industry Applications LDIA 2015*, Jul 2015.

[9] J. Ji, Z. Ling, J. Wang, W. Zhao, G. Liu, and T. Zeng, "Design and analysis of a halbach magnetized magnetic screw for artificial heart," *IEEE Transactions on Magnetics*, vol. 51, no. 11, pp. 1–4, Nov 2015.

[10] M. B. Kouhshahi and J. Z. Bird, "Analysis of a magnetically geared lead screw," in *8th Energy Conversion Congress and Exposition*, 2016.

[11] P. Campbell, “System cost analysis for an interior permanent magnet motor,” *AMES Laboratory*, Aug 2008.